

Effect of mechanical activation on dissolution kinetics of neutral leach residue of zinc calcine in sulphuric acid

Xuan-hai LI¹, Yan-juan ZHANG², Liu-ping PAN¹, Yan-song WEI³

1. School of Chemistry and Chemical Engineering, Guangxi University, Nanning 530004, China;

2. Guangxi Research Institute of Chemical Industry, Nanning 530001, China;

3. Department of Chemistry and Biology, Hechi College, Yizhou 546300, China

Received 16 April 2012; accepted 25 June 2012

Abstract: Neutral leach residue of zinc calcine (NLRZC) was mechanically activated by a stirring ball mill. Subsequently, the changes in physicochemical properties and dissolution kinetics in sulphuric acid were studied. The crystalline structure, morphology, particle size and specific surface area of the non-activated and mechanically activated NLRZC were characterized by X-ray diffraction, scanning electron microscope, particle size analyzer and volumetric adsorption analyzer, respectively. The characterization results indicate that mechanical activation (MA) induced remarkable changes in the physicochemical properties of NLRZC. The leaching experiments show that MA significantly enhances the leaching reactivity of NLRZC using the zinc extraction as evaluating index. After NLRZC is mechanically activated for 30 min and 60 min, the activation energy decreases from 56.6 kJ/mol of non-activated NLRZC to 36.1 kJ/mol and 29.9 kJ/mol, respectively. The reaction orders of the non-activated, 30 and 60 min activated NLRZC dissolution with respect to H₂SO₄ concentration were found to be 0.34, 0.30, and 0.29, respectively.

Key words: zinc; dissolution kinetics; mechanical activation; neutral leach residue

1 Introduction

Zinc sulphide minerals are considered to be the primary materials for the production of zinc from ores because the sulfides can be easily separated from gangue and concentrated by conventional flotation techniques [1,2]. Indium is commonly found to be associated with zinc sulphide ores, and indium is usually concentrated with the zinc concentrates in the flotation process [3]. So it is necessary to recover indium in the production process of zinc. The traditional hydrometallurgical extraction of zinc from its sulphides is the roast-leach-electrowinning process, which is responsible for about 80% of the total zinc production [4]. In the roasting process, zinc ferrite (franklinite, ZnFe₂O₄), a very stable phase, is easily formed when zinc oxide is in contact with the iron impurities at high temperature [5,6]. Zinc ferrite is the major zinc-bearing component in zinc calcine, and it becomes the main obstacle in the hydrometallurgical extraction of zinc because it is not

easily amenable to normal leaching [7]. Unfortunately, indium can easily enter into the crystal lattice of zinc ferrite through substituting iron to form indium-bearing zinc ferrite (ZnFe_{2-x}In_xO₄) [8,9]. After the neutral leaching process, neutral leach residue of zinc calcine (NLRZC) usually contains about 20% zinc. The zinc-bearing phases of NLRZC are mainly zinc ferrite, and also some zinc sulphides that have not converted in the roasting process. NLRZC is the main material for the recovery of indium, but the stability of zinc ferrite results in the low extraction of zinc and indium. So it is important to enhance the dissolution rate of NLRZC.

Nowadays, more and more innovative technologies are developed to recover valuable metals simply, effectively and environmentally friendly. Mechanical activation (MA), usually carried out by high-energy milling, refers to the use of mechanical actions to change the crystalline structure and physicochemical properties of the solids [10]. MA treatment of minerals represents an important contribution to different fields of solid processing technology [11–13]. In extractive metallurgy,

the oxide, sulfide and refractory minerals are activated by high energy milling, resulting in the increase of new reactive surfaces, phase transformations and deformation of crystalline structure of minerals, which may greatly enhance the reactivity of solid particles [14–16]. The increased reactivity leads to the decrease of activation energy and acceleration of leaching valuable metals present in the minerals [17–19]. TKÁČOVÁ et al [20] observed that MA could induce zinc ferrite into a metastable state and enhance the dissolution rate of zinc ferrite. BALÁŽ et al [21] investigated the leaching behavior of mechanically activated sphalerite, and found that MA treatment of sphalerite led to the increase of reaction rate and improvement of leaching selectivity. However, synthetic minerals were mainly used for theoretical studies in the previous works, while the effect of MA on the dissolution of NLRZC containing zinc ferrite and zinc sulphide has not been thoroughly discussed yet. In this study, the effect of MA on the dissolution kinetics of NLRZC in sulphuric acid was investigated, and the changes in physicochemical properties of NLRZC before and after MA were also discussed.

2 Experimental

2.1 Material

The raw NLRZC sample was obtained from Nandan, Guangxi, China. In order to remove the easily dissolvable components, the raw NLRZC was washed in 1 mol/L HCl for 20 min at 40 °C. The pretreated NLRZC was dried and sieved into different particle sizes. A size fraction of 0.075–0.096 mm (apparent particle size) was chosen in this study. The sample was characterized by X-ray diffraction (XRD) and the result is presented in Fig. 1(a), which shows that franklinite (ZnFe_2O_4), wurtzite (ZnS), anglesite (PbSO_4) and gypsum ($\text{CaSO}_4 \cdot 2\text{H}_2\text{O}$) are the major components in NLRZC. The main soluble components of NLRZC in sulphuric acid were zinc ferrite and zinc sulphide, so the leaching rate of zinc was also the dissolution rate of NLRZC. The main chemical composition (mass fraction, %) of the sample are shown as follows: 31.66% Pb, 13.76% Zn, 10.79% Fe, 6.93% Ca, 13.63% S and 0.08% In. All chemicals used in this study were of analytical grade without further purification, and deionized water was used throughout the work.

The mechanically activated NLRZC samples were prepared as follows. The non-activated NLRZC samples (50 g in each batch) were added into a ceramic chamber (2000 mL) with 1000 mL zirconia milling balls (5 mm in diameter), then mechanically activated in a stirring ball mill without other additives under ambient atmosphere. Milling was carried out at 500 r/min for all the batch

experiments. The samples were activated for 30 and 60 min in separate experiments. The resulting samples were sealed for characterization and leaching experiments.

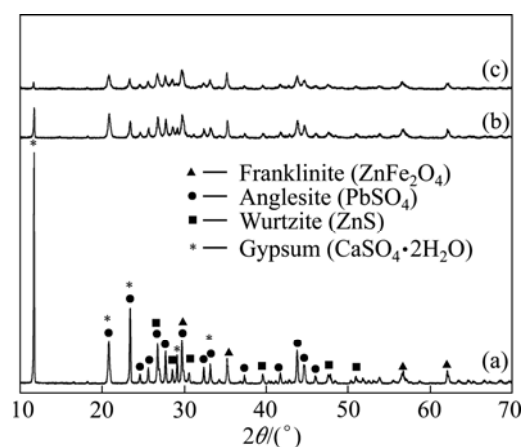


Fig. 1 XRD patterns of NLRZC: (a) Non-activated; (b) 30 min activated; (c) 60 min activated

2.2 Characterization

XRD analysis of the nonactivated and activated NLRZC samples was carried out using Rigaku D/MAX 2500 V diffractometer (Japan) at 40 kV and 30 mA, with a step size of 0.02° and a recorded range from 10° to 70° . The effect of MA was evaluated by an increase in mineral amorphization (A , the degree of mineral disordering) compared with the reference sample (non-activated), which was assumed to correspond to 0 amorphization. The value of A was calculated using the following equation:

$$A = \left(1 - \frac{U_0}{I_0} \cdot \frac{I_x}{U_x} \right) \times 100\% \quad (1)$$

where U_0 and U_x denote the backgrounds of the reference sample (non-activated sample) and activated samples; I_0 and I_x are integral intensities of diffraction lines of the reference sample and activated samples, respectively [22].

The morphology was examined by a scanning electron microscope (SEM, S-570, Hitachi, Japan). Particle size analysis was measured using a laser diffraction particle size analyzer (Malvern, Mastersizer 2000, UK). Specific surface area (S_A) was determined by the Brunauer, Emmett and Teller (BET) method in a volumetric adsorption analyzer (Micromeritics, ASAP 2020 M, USA).

2.3 Leaching experiment

Leaching experiments were carried out in 1000 mL three-neck flask which was immersed in a thermostatically controlled water bath, and the experiments were equipped with reflux condenser, mechanical stirrer, thermometer and sampling device. In

each experiment, the three-neck flask with 600 mL of sulfuric acid solution was preheated, and then 6.0 g sample was added when the temperature reached the pre-set value and the mixture was stirred at 500 r/min. The zinc-bearing phases reacted according to the following equations:



Aliquots (~5 mL) of the solution were withdrawn at appropriate time intervals to determine the Zn^{2+} concentration using EDTA titration method. In these experiments, the solid/liquid ratio, reaction temperature, and sulphuric acid concentration were fixed at 10 g/L, 80 °C, and 1.5 mol/L, respectively.

3 Results and discussion

3.1 Influence of MA on physicochemical properties of NLRZC

The XRD patterns of the non-activated and mechanically activated NLRZC samples are illustrated in Fig. 1. As seen in Fig. 1, there are no new peaks observed after MA, indicating that no phase change occurred during milling. But the intensity of diffraction lines decreased and the diffraction peaks broadened with the increase of activation time. It demonstrates that the decrease in crystalline phase, the variation of crystallite size and the lattice distortion are linked with ball impacts and collisions [23]. The amorphization, which is a measure of the crystallographic disorder of the structure, was calculated according to Eq. (1) for the (311) plane ($2\theta \approx 35.3^\circ$) of zinc ferrite in activated samples. After 30 and 60 min milling, the amorphization of zinc ferrite phase increased from 0 to 29.0% and 53.7%, respectively. It shows that MA caused obvious changes in the crystal structure of NLRZC.

Figure 2 shows the morphologies of the unmilled sample and samples milled for various time, respectively. The NLRZC initially consisted of incompact particles which have different sizes. The particles were broken into much smaller ones with the grain size below 1 μm after 30 min milling, but the formation of aggregates can be observed clearly after 60 min milling. The amorphous substance covering the surface of large particles can also be seen in the SEM images of the activated NLRZC samples, especially the 60 min milled one. The generation of amorphous substance demonstrates that the crystalline structure was deformed and the fresh surface was generated during milling.

The particle size and S_A of NLRZC samples are shown in Table 1. The original NLRZC was composed of

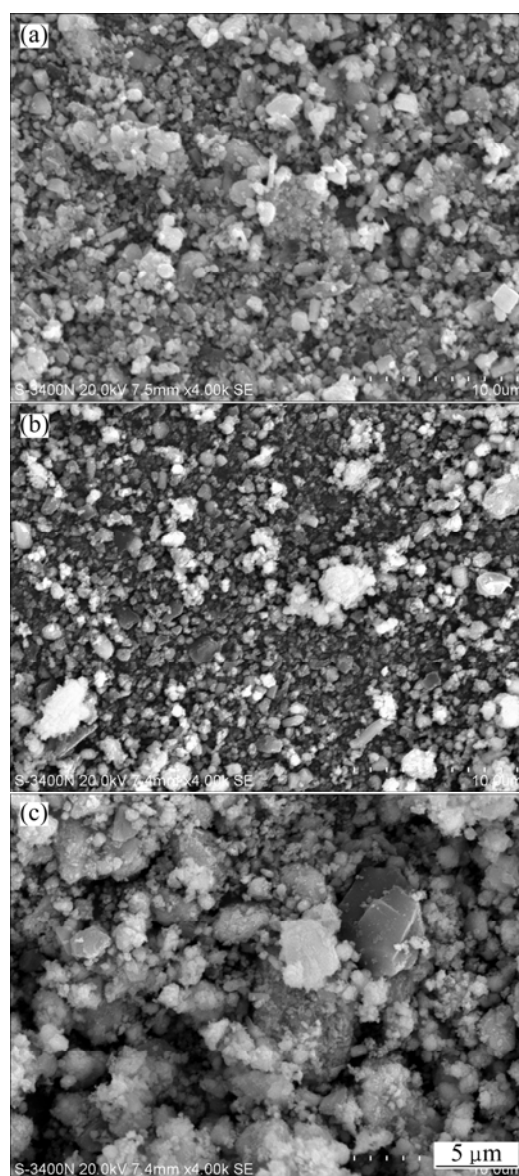


Fig. 2 SEM images of NLRZC: (a) Non-activated; (b) 30 min activated; (c) 60 min activated

particles with the median particle size ($d_{0.5}$) around 4.3 μm . After 30 min milling, the particle size decreased significantly, and a number of small grains with the particle size of less than 0.1 μm generated. But longer activation time (60 min) essentially had a minor effect on the particle size. The $d_{0.5}$ of NLRZC activated for 60 min increased from 3.2 μm (30 min) to 4.1 μm and the small grains gradually aggregated into large particles, which were consistent with the foregoing statements regarding the morphology analysis. The S_A of NLRZC increased when the sample was milled for 30 min, but decreased after 60 min milling. This can be considered to be due to the combination of two processes: breakage and rewelding [24]. In the early stage, the particles were broken at a high rate and the rewelding was relatively

minor. As the milling time increased continuously, the rate of particle agglomeration gradually exceeded that of particle breakage, which increased the particle size and decreased the S_A .

Table 1 Particle size and S_A of non-activated NLRZC and samples activated for different time

Activation time/min	$d_{0.1}/\mu\text{m}$	$d_{0.5}/\mu\text{m}$	$d_{0.9}/\mu\text{m}$	$S_A/(\text{m}^2\cdot\text{g}^{-1})$
0	1.4	4.3	16.3	14.36
30	0.1	3.2	12.0	18.58
60	0.7	4.1	16.2	15.50

3.2 Effect of MA on dissolution of NLRZC

The effect of MA on NLRZC dissolution was studied by varying the activation time from 0 to 60 min, and the results are shown in Fig. 3. It can be observed that after being activated for 30 and 60 min, the leaching efficiency of zinc increased from 43.8% (non-activated) to 57.6% and 64.7%, respectively. The XRD, morphology, particle size, and S_A analyses show that the changes in physicochemical property of NLRZC are significant after MA, which can efficiently enhance the reactivity of NLRZC. Therefore, the increase of zinc extraction can be attributed to the increased reactivity of zinc ferrite and zinc sulphide, which results from lattice defect, structural disorder, and the generation of fresh, previously unexposed surfaces in NLRZC induced by the MA pretreatment. Therefore, it can be concluded that the effect of MA on the dissolution of NLRZC is significant.

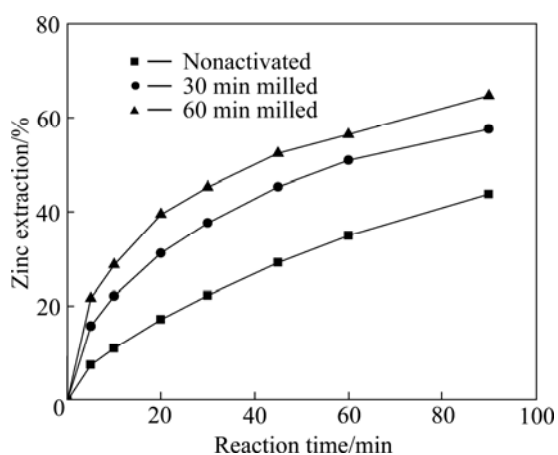


Fig. 3 Effect of MA on zinc extraction from NLRZC (80 °C; 1.5 mol/L H_2SO_4 ; solid/liquid ratio 10 g/L; stirring speed 500 r/min)

3.3 Effect of reaction temperature

The influence of reaction temperature on the dissolution of unmilled and milled NLRZC samples under certain reaction conditions was investigated in the range of 70 to 90 °C. The results in Fig. 4 show that the reaction temperature has a noticeable effect on the

dissolution rate of NLRZC, and the zinc extraction from all these samples increases with the increase of reaction temperature. It can also be observed that the dependency of zinc leaching efficiency on temperature decreases as the activation time increases.

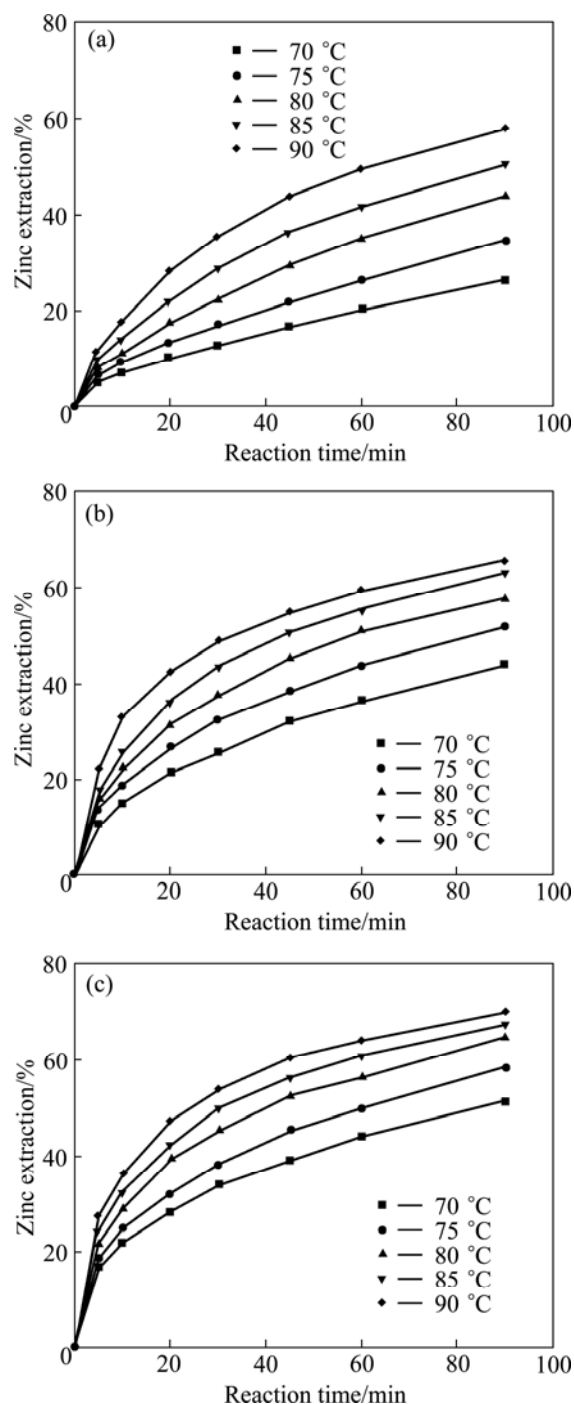


Fig. 4 Effect of temperature on zinc extraction from NLRZC: (a) Non-activated; (b) 30 min milled; (c) 60 min milled

3.4 Effect of sulphuric acid concentration

A series of leaching experiments were carried out at different initial H_2SO_4 concentrations, ranging from 0.5 to 2.5 mol/L. As seen in Fig. 5, the increase of acid concentration increased the leaching rate of zinc, but

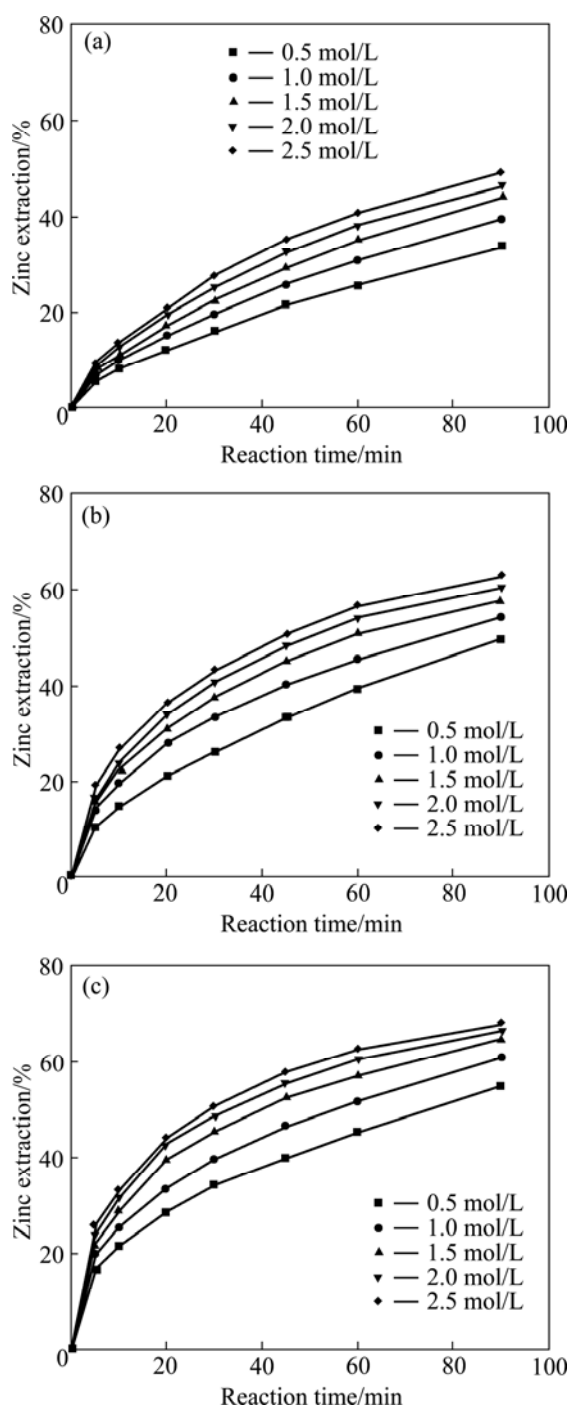


Fig. 5 Effect of H_2SO_4 concentration on zinc extraction from NLRZC: (a) Non-activated; (b) 30 min milled; (c) 60 min milled

the increasing trend was not very obvious for all these non-activated and activated NLRZC samples. After leaching for 90 min, the zinc leaching rate of non-activated, 30 and 60 min milled samples increased from 33.7%, 49.8%, and 54.8% to 49.1%, 62.8%, and 67.9%, respectively, when the concentration of H_2SO_4 was increased from 0.5 mol/L to 2.5 mol/L. Therefore, the effect of H_2SO_4 concentration on extracting zinc from NLRZC was not very remarkable.

3.5 Kinetic modelling

The dissolution of NLRZC in sulphuric acid belongs to the noncatalytic fluid-solid reaction model. For many of the noncatalytic fluid-solid reactions, shrinking core model has been used [25,26]. The basic assumption of shrinking core model is that the particles are spheres with the same radius [27]. From the SEM images of NLRZC, it can be seen that the samples were easily agglomerated, and the apparent particle size was not the real particle size because it was impossible to sieve the NLRZC into single size sample. So it is not suitable to explain this reaction using the shrinking core model. The semi-empirical Avrami-Erofeev equation, $-\ln(1-\alpha) = kt^n$, was chosen to express these kinetic data [28]. The values of n were calculated using the experimental data presented in Figs. 4 and 5. The values of n for the non-activated, 30 and 60 min activated samples were determined to be 0.677, 0.562 and 0.490, respectively. The equations for non-activated and two activated samples can be written as follows:

$$-\ln(1-\alpha) = kt^{0.677} \quad (\text{non-activated}) \quad (4)$$

$$-\ln(1-\alpha) = kt^{0.562} \quad (\text{activated for 30 min}) \quad (5)$$

$$-\ln(1-\alpha) = kt^{0.490} \quad (\text{activated for 60 min}) \quad (6)$$

where α is the fraction reacted, k is the rate constant, t is the reaction time. The value of parameter n may indicate the nature of the controlling step, which is independent of process conditions [29]. The decrease of n value demonstrates that MA could accelerate the reaction rate and the chemical reaction is not the main controlling step in the dissolution of activated NLRZC.

3.6 Evaluation of activation energy

In order to determine the activation energies of the non-activated and activated NLRZC samples, Eqs. (4), (5) and (6) were applied to the data obtained from each temperature in Fig. 4. Figure 6 shows the fitting of three selected models to the experimental data. It is readily noted that these models fit the kinetic data of leaching experiments very well. Figure 7 presents the Arrhenius plot constructed with the rate constant values at different temperatures, k_T , calculated from the data in Fig. 6. The activation energies of non-activated, 30 and 60 min activated NLRZC samples were determined to be 56.6, 36.1, and 29.9 kJ/mol, respectively. The decrease in activation energy indicates that chemical reaction control was gradually replaced by diffusion control, which became the main controlling step in the dissolution of activated NLRZC [18].

It is known that the kinetics of heterogeneous reaction is determined not only by the contact area but also by the structure of the mineral. The required modification of this structure can be achieved by MA of the minerals, as a rule by intensive milling [30]. The

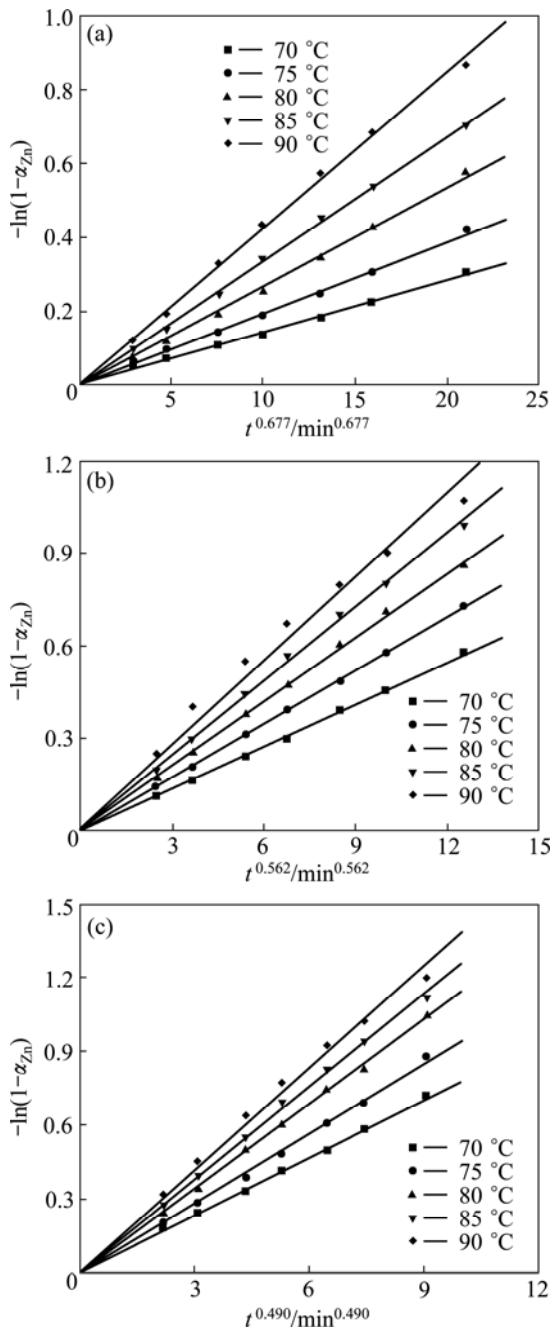


Fig. 6 Plots of $-\ln(1-\alpha)$ vs $t^{0.677}$, $t^{0.562}$, $t^{0.490}$ for NLRZC at various reaction temperatures: (a) Non-activated; (b) 30 min milled; (c) 60 min milled

defect and disorder in the crystalline lattice of the mineral bring about a decrease (ΔE^*) in activation energy:

$$\Delta E^* = E - E^* \quad (7)$$

where E is the activation energy of the non-activated mineral and E^* is the activation energy of the activated mineral.

The rate constant of activated mineral (k^*) can be described by using the Arrhenius equation:

$$k^* = k \exp(\Delta E^*/RT) \quad (8)$$

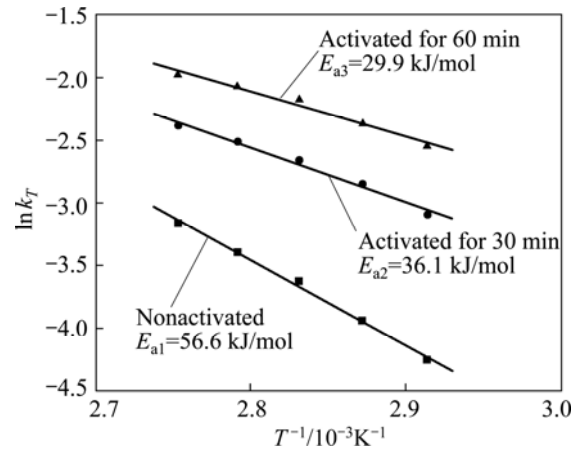


Fig. 7 Arrhenius plot for non-activated and activated NLRZC

where k , R and T stand for rate constant of unmilled mineral, gas constant and leaching temperature, respectively.

As $\Delta E^* > 0$, then $\exp(\Delta E^*/RT) > 1$ and thus it follows Eq. (8) that $k^* > k$. The activation energy of NLRZC dissolution in H_2SO_4 decreases obviously after MA, which demonstrates that the leaching rate of activated samples was greater than that of the non-activated sample. So MA significantly enhanced the reactivity of NLRZC, and the leaching reaction became less sensitive to temperature.

3.7 Evaluation of reaction order

The use of these three kinetic models also allows for the determination of the reaction orders with respect to H_2SO_4 concentration. Similarly, according to the kinetic data of leaching experiments in Fig. 5, the apparent reaction orders for the dissolution of non-activated, 30 and 60 min activated NLRZC samples were found proportional to 0.34, 0.30, and 0.29 power of H_2SO_4 concentration, respectively, which are presented in Fig. 8.

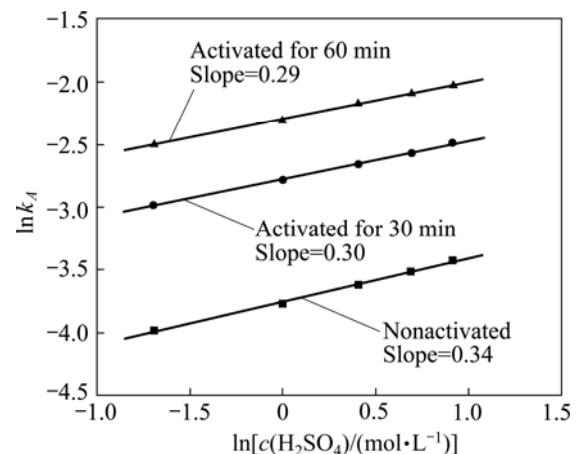


Fig. 8 Determination of reaction order for non-activated and activated NLRZC with respect to H_2SO_4 concentration

The results show that the effect of H_2SO_4 concentration on the dissolution of non-activated NLRZC was not significant, so it was difficult to greatly decrease the dependency of zinc extraction on H_2SO_4 concentration by MA.

4 Conclusions

1) The characterization of the non-activated and activated NLRZC samples shows that MA causes the decrease in particle size, the variation of morphology, and the increase in specific surface area and amorphization. But the particles agglomeration causes the increase in particle size and decrease in specific surface area when prolonging the milling time from 30 to 60 min.

2) The leaching experiments show that MA not only significantly improves the dissolution rate of NLRZC, but also decreases the dependency of NLRZC dissolution on temperature.

3) The activation energies of the non-activated, 30 and 60 min activated NLRZC are calculated to be 56.6, 36.1 and 29.9 kJ/mol, respectively, which also indicates that MA accelerates the dissolution rate of NLRZC and the leaching reaction becomes less sensitive to temperature.

4) The apparent reaction orders for the dissolution reaction of the unmilled, 30 and 60 min milled samples with respect to H_2SO_4 concentration are 0.34, 0.30 and 0.29, respectively, which indicates that H_2SO_4 concentration has no very remarkable effect on the dissolution of all these three NLRZC samples.

References

- [1] ZHANG C L, ZHAO Y C, GUO C X, HUANG X, LI H J. Leaching of zinc sulfide in alkaline solution via chemical conversion with lead carbonate [J]. *Hydrometallurgy*, 2008, 90(1): 19–25.
- [2] HUANG Wei, XIE Song-ming. Test and research on reduction roasting process of zinc calcine [J]. *Non-ferrous Smelting*, 2008, 29(4): 31–33. (in Chinese)
- [3] TONG Xiong, SONG Shao-xian, HE Jian, LOPEZ-VALDIVIESO Alejandro. Flotation of indium-bearing marmatite from multi-metallic ore [J]. *Rare Metals*, 2008, 27(2): 107–111.
- [4] AL-HARAHSEH M, KINGMAN S. The influence of microwaves on the leaching of sphalerite in ferric chloride [J]. *Chemical Engineering and Processing: Process Intensification*, 2007, 46(10): 883–888.
- [5] HOLLOWAY P C, ETSSELL T H, MURLAND A L. Roasting of La oroya zinc ferrite with Na_2CO_3 [J]. *Metallurgical and Materials Transactions B*, 2007, 38(5): 781–791.
- [6] LI Xi-ming, CHEN Jia-yong, KAMMEL Roland, PAWELK Franz. Effect of mechanical activation by fine grinding on leaching behaviour of zinc ferrite [J]. *Nonferrous Metals*, 1991, 43(2): 44–48. (in Chinese)
- [7] SWARNKAR S R, GUPTA B L, SEKHARAN R D. Iron control in zinc plant residue leach solution [J]. *Hydrometallurgy*, 1996, 42(1): 21–26.
- [8] RAO B P, RAO K H. Distribution of In^{3+} ions in indium-substituted Ni–Zn–Ti ferrites [J]. *Journal of Magnetism and Magnetic Materials*, 2005, 292: 44–48.
- [9] ZHANG Y J, LI X H, PAN L P, LIANG X Y, LI X P. Studies on the kinetics of zinc and indium extraction from indium-bearing zinc ferrite [J]. *Hydrometallurgy*, 2010, 100(3–4): 172–176.
- [10] BALÁŽ P. Mechanical activation in hydrometallurgy [J]. *International Journal of Mineral Processing*, 2003, 72(1–4): 341–354.
- [11] ZHAO Z, LONG S, CHEN A, HUO G, LI H, JIA X, CHEN X. Mechanochemical leaching of refractory zinc silicate (hemimorphite) in alkaline solution [J]. *Hydrometallurgy*, 2009, 99(3–4): 255–258.
- [12] HU Hui-ping, CHEN Qi-yuan, YIN Zhou-lan, HE Yue-hui, HUANG Bai-yun. Mechanism of mechanical activation for sulfide ores [J]. *Transactions of Nonferrous Metals Society of China*, 2007, 17(1): 205–213.
- [13] ZHANG Yang, ZHENG Shi-li, DU Hao, XU Hong-bin, ZHANG Yi. Effect of mechanical activation on alkali leaching of chromite ore [J]. *Transactions of Nonferrous Metals Society of China*, 2010, 20(5): 888–891.
- [14] BALÁŽ P, ACHIMOVIČOVÁ M. Selective leaching of antimony and arsenic from mechanically activated tetrahedrite, jamesonite and enargite [J]. *International Journal of Mineral Processing*, 2006, 81(1): 44–50.
- [15] ZHANG L, HU H, WEI L, CHEN Q, TAN J. Effects of mechanical activation on the HCl leaching behavior of titanite, ilmenite, and their mixtures [J]. *Metallurgical and Materials Transactions B*, 2010, 41(6): 1158–1165.
- [16] CAO Qin-Yuan, LI Jie, CHEN Qi-Yuan. Effects of mechanical activation on alkaline leaching and physicochemical properties of hemimorphite [J]. *The Chinese Journal of Nonferrous Metals*, 2010, 20(2): 354–362. (in Chinese)
- [17] FICERIOVÁ J, BALÁŽ P, BOLDIŽÁROVÁ E, JELEŇ S. Thiosulfate leaching of gold from a mechanically activated CuPbZn concentrate [J]. *Hydrometallurgy*, 2002, 67(1–3): 37–43.
- [18] ZHANG Y J, LI X H, PAN L P, WEI Y S, LIANG X Y. Effect of mechanical activation on the kinetics of extracting indium from indium-bearing zinc ferrite [J]. *Hydrometallurgy*, 2010, 102(1–4): 95–100.
- [19] ZHANG Yan-juan, LI Xuan-hai, PAN Liu-ping, WEI Yan-song. Influences of mechanical activation on dissolution kinetics and physicochemical properties of indium-bearing zinc ferrite [J]. *The Chinese Journal of Nonferrous Metals*, 2012, 22(1): 315–323. (in Chinese)
- [20] TKÁČOVÁ K, ŠEPELÁK V, ŠTEVULOVÁ N, BOLDYREV V V. Structure-reactivity study of mechanically activated zinc ferrite [J]. *Journal of Solid State Chemistry*, 1996, 123(1): 100–108.
- [21] BALÁŽ P, ALÁČOVÁ A, ACHIMOVIČOVÁ M, FICERIOVÁ J, GODOČÍKOVÁ E. Mechanochemistry in hydrometallurgy of sulphide minerals [J]. *Hydrometallurgy*, 2005, 77(1–2): 9–17.
- [22] BALÁŽ P, ALÁČOVÁ A, BRIANČIN J. Sensitivity of Freundlich equation constant $1/n$ for zinc sorption on changes induced in calcite by mechanical activation [J]. *Chemical Engineering Journal*, 2005, 114(1–3): 115–121.
- [23] EBRAHIMI-KAHRIZSANGI R, ABBASI M H, SAIDI A. Mechanochemical effects on the molybdenite roasting kinetics [J]. *Chemical Engineering Journal*, 2006, 121(2–3): 65–71.
- [24] YUAN T C, CAO Q Y, LI J. Effects of mechanical activation on physicochemical properties and alkaline leaching of hemimorphite [J]. *Hydrometallurgy*, 2010, 104(2): 136–141.
- [25] ASHRAF M, ZAFAR Z I, ANSARI T M. Selective leaching kinetics and upgrading of low-grade calcareous phosphate rock in succinic acid [J]. *Hydrometallurgy*, 2005, 80(4): 286–292.

- [26] SOUZA A D, PINA P S, LIMA E V O, SILVA C A D, LEÃO V A. Kinetics of sulphuric acid leaching of a zinc silicate calcine [J]. Hydrometallurgy, 2007, 89(3–4): 337–345.
- [27] VELARDO A, GIONA M, ADROVER A, PAGNANELLI F, TORO L. Two-layer shrinking-core model: Parameter estimation for the reaction order in leaching processes [J]. Chemical Engineering Journal, 2002, 90(3): 231–240.
- [28] OKUR H, TEKIN T, OZER A K, BAYRAMOGLU M. Effect of ultrasound on the dissolution of colemanite in H_2SO_4 [J]. Hydrometallurgy, 2002, 67(1–3): 79–86.
- [29] SOKIĆ M D, MARKOVIĆ B, ŽIVKOVIĆ D. Kinetics of chalcocopyrite leaching by sodium nitrate in sulphuric acid [J]. Hydrometallurgy, 2009, 95(3–4): 273–279.
- [30] BALÁŽ P, BRIANČIN J, ŠEPELÁK V, HAVLÍK T, ŠKROBIAN M. Non-oxidative leaching of mechanically activated stibnite [J]. Hydrometallurgy, 1992, 31(3): 201–212.

机械活化对锌焙砂中浸渣硫酸溶解动力学的影响

黎铨海¹, 张燕娟², 潘柳萍¹, 韦岩松³

1. 广西大学 化学化工学院, 南宁 530004;
2. 广西壮族自治区化工研究院, 南宁 530001;
3. 河池学院 化生系, 宜州 546300

摘 要: 采用搅拌球磨对锌焙砂中浸渣(中浸渣)进行机械活化, 研究机械活化对中浸渣的物化性质以及在硫酸溶液中溶解动力学的影响。采用 X 射线衍射仪、扫描电镜、激光粒度分析仪和比表面积分析仪, 分析活化前后中浸渣的晶体结构、表观形貌、粒度和比表面积的变化规律。结果表明: 机械活化使中浸渣的物化性质发生明显改变。以锌的浸出率为评价指标, 浸出实验结果表明: 机械活化可显著提高中浸渣的反应活性。经机械活化 30 和 60 min 后, 中浸渣在硫酸中溶解的表现活化能由未活化时的 56.6 kJ/mol 分别降至 36.1 kJ/mol 和 29.9 kJ/mol。未活化、活化 30 min 和 60 min 的中浸渣相对于硫酸浓度的表现反应级数分别为 0.34、0.30 和 0.29。

关键词: 锌; 溶解动力学; 机械活化; 中浸渣

(Edited by Chao WANG)